PROBLEMS IN NONLINEAR ACOUSTICS:

RAYLEIGH WAVES, PULSED SOUND BEAMS, REFLECTION OF FOCUSED BEAMS, WAVEGUIDES, COOPERATIVE RADIATION OF SOUND BY BUBBLES, ACOUSTIC STREAMING EFFECTS IN STANDING WAVES, AND SPARK-SOURCE LITHOTRIPTER PULSES

Mark F. Hamilton

DEPARTMENT OF MECHANICAL ENGINEERING
THE UNIVERSITY OF TEXAS AT AUSTIN
AUSTIN, TEXAS 78712-1063

14 August 1992

Fourth Annual Summary Report
ONR Grant N00014-89-J-1003

Prepared for:

OFFICE OF NAVAL RESEARCH
DEPARTMENT OF THE NAVY
ARLINGTON, VA 22217-5000

UNCLASSIFIED
SECURITY CLASSIFICATION OF THIS PAGE

REPORT DOCUMENTATION PAGE

Form Approved OMB No. 0704-0188

1a REPORT SECURITY CLASSIFICATION: Unclassified	1b RESTRICTIVE MARKINGS
2a SECURITY CLASSIFICATION AUTHORITY	3 DISTRIBUTION / AVAILABILITY OF REPORT: Approved for public release; distribution unlimited
2b DECLASSIFICATION / DOWNGRADING SCHEDULE	
4 PERFORMING ORGANIZATION REPORT NUMBER(S): ASR-4	5 MONITORING ORGANIZATION REPORT NUMBER(S)
6a NAME OF PERFORMING ORGANIZATION: University of Texas; 6b OFFICE SYMBOL (If applicable)	7a NAME OF MONITORING ORGANIZATION: Office of Naval Research
6c ADDRESS (City, State, and ZIP Code): Department of Mechanical Engineering, The University of Texas at Austin, Austin, TX 78712-1063	7b ADDRESS (City, State, and ZIP Code): Physics Division, Code 1112, Arlington, VA 22217-5000
8a NAME OF FUNDING / SPONSORING ORGANIZATION; 8b OFFICE SYMBOL (If applicable)	9 PROCUREMENT INSTRUMENT IDENTIFICATION NUMBER: N00014-89-J-1003
8c ADDRESS (City, State, and ZIP Code)	10 SOURCE OF FUNDING NUMBERS: PROGRAM ELEMENT NO. 61153N; PROJECT NO. 4126943; TASK NO.; WORK UNIT ACCESSION NO.

11 TITLE (Include Security Classification): Problems in Nonlinear Acoustics

12 PERSONAL AUTHOR(S): Mark F. Hamilton

13a TYPE OF REPORT	13b TIME COVERED	14 DATE OF REPORT (Year, Month, Day)	15 PAGE COUNT
Annual Summary	FROM 910801 TO 920814	920814	29

16 SUPPLEMENTARY NOTATION

17 COSATI CODES			18 SUBJECT TERMS (Continue on reverse if necessary and identify by block number)
FIELD	GROUP	SUB-GROUP	nonlinear acoustics, waveguides, pulsed beams, layered media, focused beams, surface waves
20	01		

19 ABSTRACT (Continue on reverse if necessary and identify by block number)

Nine projects are discussed in this annual summary report, all of which involve basic research in physical acoustics, mainly nonlinear acoustics: (1) Nonlinear Rayleigh Waves, (2) Finite Amplitude Pulses in Liquids with Strong Absorption, (3) Reflection of a Focused Beam from a Curved Target, (4) Finite Amplitude Propagation in a Sound Velocity Channel, (5) Second Harmonic Generation in Pekeris Waveguides, (6) Finite Amplitude Propagation in Multiple Waveguide Modes, (7) Cooperative Radiation and Scattering of Sound by Bubbles, (8) Water Fountains Produced by Intense Standing Waves in Air, and (9) Spark-Source Lithotripter Pulses.

20 DISTRIBUTION / AVAILABILITY OF ABSTRACT: ☒ UNCLASSIFIED/UNLIMITED ☐ SAME AS RPT ☐ DTIC USERS	21 ABSTRACT SECURITY CLASSIFICATION: Unclassified
22a NAME OF RESPONSIBLE INDIVIDUAL: L. E. Hargrove, ONR Physics Division	22b TELEPHONE (Include Area Code): (703) 696-4221; 22c OFFICE SYMBOL: ONR Code 1112

DD Form 1473, JUN 86 *Previous editions are obsolete.*

SECURITY CLASSIFICATION OF THIS PAGE

UNCLASSIFIED

CONTENTS

INTRODUCTION

This annual summary report describes research performed from 1 August 1991 through 14 August 1992 with support from ONR under grant N00014-89-J-1003. The following projects are discussed in this report:

I. Nonlinear Rayleigh Waves

II. Finite Amplitude Pulses in Liquids with Strong Absorption

III. Reflection of a Focused Beam from a Curved Target

IV. Finite Amplitude Propagation in a Sound Velocity Channel

V. Second Harmonic Generation in Pekeris Waveguides

VI. Finite Amplitude Propagation in Multiple Waveguide Modes

VII. Cooperative Radiation and Scattering of Sound by Bubbles

VIII. Water Fountains Produced by Intense Standing Waves in Air

IX. Spark-Source Lithotripter Pulses

Contributions to these projects were made by the following individuals:

Senior Personnel

- M. F. Hamilton, principal investigator
- Yu. A. Il'insky, visiting scientist
- E. A. Zabolotskaya, visiting scientist

Graduate Students

- M. A. Averkiou, Ph.D. student in Mechanical Engineering
- C. E. Bruch, M.A. student in Physics
- Y.-S. Lee, Ph.D. student in Mechanical Engineering
- D. E. Reckamp, M.S. student in Mechanical Engineering
- D. J. Shull, M.S. student in Electrical Engineering
- T. W. VanDoren, Ph.D. student in Mechanical Engineering

Professor Il'insky and Academician Zabolotskaya, on leave from the Physics Department of Moscow University and from the General Physics Institute in Moscow, respectively, joined our acoustics group in September 1991. Professor Il'insky returned to Moscow in June 1992. Their main source of financial support was the David and Lucile Packard Foundation Fellowship for Science and Engineering. The graduate students received partial financial support from several funding agencies, as noted in the relevant sections.

The following manuscripts and abstracts, which describe work supported at least in part by ONR, have been published (or submitted for publication) since 1 August 1991.

Refereed Journals

- M. F. Hamilton and E. A. Zabolotskaya, "Nonlinear propagation of sound in a liquid layer between a rigid and a free surface," *J. Acoust. Soc. Am.* **90**, 1048–1055 (1991).

- M. F. Hamilton, "Comparison of three transient solutions for the axial pressure in a focused sound beam," *J. Acoust. Soc. Am.* **92**, 527–532 (1992).

- C. M. Darvennes and M. F. Hamilton, "Additional remarks on parametric reception near a reflecting plane," *J. Acoust. Soc. Am.* (in press).

- Yu. A. Il'insky, and E. A. Zabolotskaya, "Cooperative radiation and scattering of acoustic waves by gas bubbles in liquids," *J. Acoust. Soc. Am.* (in press).

- M. F. Hamilton, "A transient axial solution for the reflection of a spherical wave from a concave ellipsoidal mirror," *J. Acoust. Soc. Am.* (in review).

- M. F. Hamilton, Yu. A. Il'insky, and E. A. Zabolotskaya, "On the existence of stationary nonlinear Rayleigh waves," *J. Acoust. Soc. Am.* (in review).

Conference Proceedings

- M. F. Hamilton, "A transient solution for the axial pressure field of a spark-source lithotripter," to appear in *Proceedings of the 14th International Congress on Acoustics* (Beijing, China, September 1992).

Oral Presentation Abstracts

- M. F. Hamilton, "An axial solution for the reflection of a spherical wave from a concave ellipsoidal mirror," *J. Acoust. Soc. Am.* **90**, 2340 (1991).

- T. W. VanDoren and M. F. Hamilton, "Water fountains produced by intense standing waves in air," *J. Acoust. Soc. Am.* **91**, 2330 (1992).

- Yu. A. Il'insky and E. A. Zabolotskaya, "Cooperative radiation of acoustic waves by gas bubbles in a liquid," *J. Acoust. Soc. Am.* **91**, 2351 (1992).
- D. E. Reckamp, E. A. Zabolotskaya, and M. F. Hamilton, "Propagation of finite amplitude sound in a waveguide with a parabolic sound velocity profile," *J. Acoust. Soc. Am.* **91**, 2352 (1992).
- M. A. Averkiou, Y.-S. Lee, and M. F. Hamilton, "Propagation of pulsed finite amplitude sound beams in a liquid with strong absorption," *J. Acoust. Soc. Am.* **91**, 2455 (1992).
- M. A. Averkiou and M. F. Hamilton, "Reflection of focused sound beams from curved surfaces," *J. Acoust. Soc. Am.* **91**, 2470 (1992).

Theses

- D. E. Reckamp, "Propagation of finite amplitude sound in a waveguide with a parabolic sound velocity profile," M.S. Thesis, The University of Texas at Austin (May 1992).

I. Nonlinear Rayleigh Waves

This work was performed by Yu. A. Il'insky, D. J. Shull, and E. A. Zabolotskaya. Additional financial support was provided by the Packard Foundation. Computing resources were provided by The University of Texas System Center for High Performance Computing.

Rayleigh waves are combinations of P waves (compressional waves) and S waves (shear waves) that propagate along free surfaces of elastic solids. Because their energy is confined within a layer having a thickness of approximately one wavelength, Rayleigh waves experience relatively small spreading losses as compared with unbounded P and S waves (i.e., cylindrical as opposed to spherical spreading). Rayleigh waves therefore transport energy from earthquakes and underground explosions over large distances in the earth, often several times around. Also, the ease with which Rayleigh waves can be generated and detected by electrodes on the surfaces of piezoelectric materials, and the fact that their propagation speed is independent of frequency, have led to the widespread use of Rayleigh waves for performing various analog signal processing functions (e.g., delay lines, filters, and Fourier transforms) at megahertz frequencies.

A new theoretical model for the propagation of nonlinear Rayleigh waves has been developed recently by Zabolotskaya.[1] The model is based on Hamiltonian formalism, and it yields a set of coupled equations that may be written in the dimensionless form

$$\frac{dV_n}{dR} + \left(\frac{m}{2R} + A_n\right)V_n = 2n^2 \sum_{m=n+1}^{N} C_{m,m-n} V_m V_{m-n}^* - n^2 \sum_{m=1}^{n-1} C_{m,n-m} V_m V_{n-m} \qquad (1)$$

where V_n is a complex spectral amplitude in a Fourier series representation of the velocity waveform, R is distance, A_n are frequency dependent attenuation coefficients, and C_{mn} are nonlinearity coefficients that depend on the individual spectral interactions. Equation (1) applies to plane waves for $m = 0$ and to cylindrical waves for $m = 1$. Three investigations based on Eq. (1) are discussed in this section.

The first investigation concentrates on the properties of harmonic generation in nonlinear Rayleigh waves. The previous analysis by Zabolotskaya[1] focused on distortion of the time waveform. Quasilinear solutions have now been derived for second harmonic generation in plane and cylindrical Rayleigh waves that propagate in isotropic solids with arbitrary attenuation properties. The quasilinear solutions were used to derive expressions for the finite amplitude losses at the source frequency (following the very successful analysis by Merklinger for finite amplitude sound in thermoviscous fluids[2]). For brevity, we present here only the approximate analytical solutions for the source frequency component for the case of negligible small signal attenuation (i.e., for which losses occur mainly at the shocks):

$$V_1 = \frac{1}{\sqrt{1 + 8C_{11}^2 R^2}} \qquad m = 0 \qquad \text{(plane)} \tag{2}$$

$$= \frac{\sqrt{R_0/R}}{\sqrt{1 + 32C_{11}^2 R_0(\sqrt{R} - \sqrt{R_0})^2}} \qquad m = 1 \qquad \text{(cylindrical)} \tag{3}$$

The source is at $R = 0$ for plane waves and $R = R_0$ for cylindrical waves. The above expressions are found to be in good agreement with the numerical solutions obtained from Eq. (1), even well into the shock wave region. Note that the source frequency components for both plane and cylindrical waves in the shock wave region (large R) are attenuated at the same rate (as R^{-1}). Both plane and cylindrical Rayleigh waves are found to experience saturation, whereby the wave amplitude at a fixed field point no longer increases with source level for source levels sufficiently high that shock waves are produced near the source.

In Fig. 1 is shown the distortion and eventual acoustic saturation of an initially monofrequency, planar Rayleigh wave in steel as a function of source level. The spectra and waveforms are normalized by their values at the source, and the field point is at a fixed distance from the source. Figures in the same row correspond to the same normalized source level L_0, and successive rows correspond to increasing source level. The first column reveals the harmonic generation that accompanies propagation as the source level is increased. The second column reveals the distortion of the horizontal velocity waveform. At $L_0 = 30$ dB the waveform exhibits the sawtooth profile that is characteristic of finite amplitude sound in fluids. At $L_0 = 40$ dB, however, cusps appear at the beginning and end of the shock front. The peak amplitudes at these cusps generally exceed the amplitude of the source waveform. Since the depth penetration of a Rayleigh wave is inversely proportional

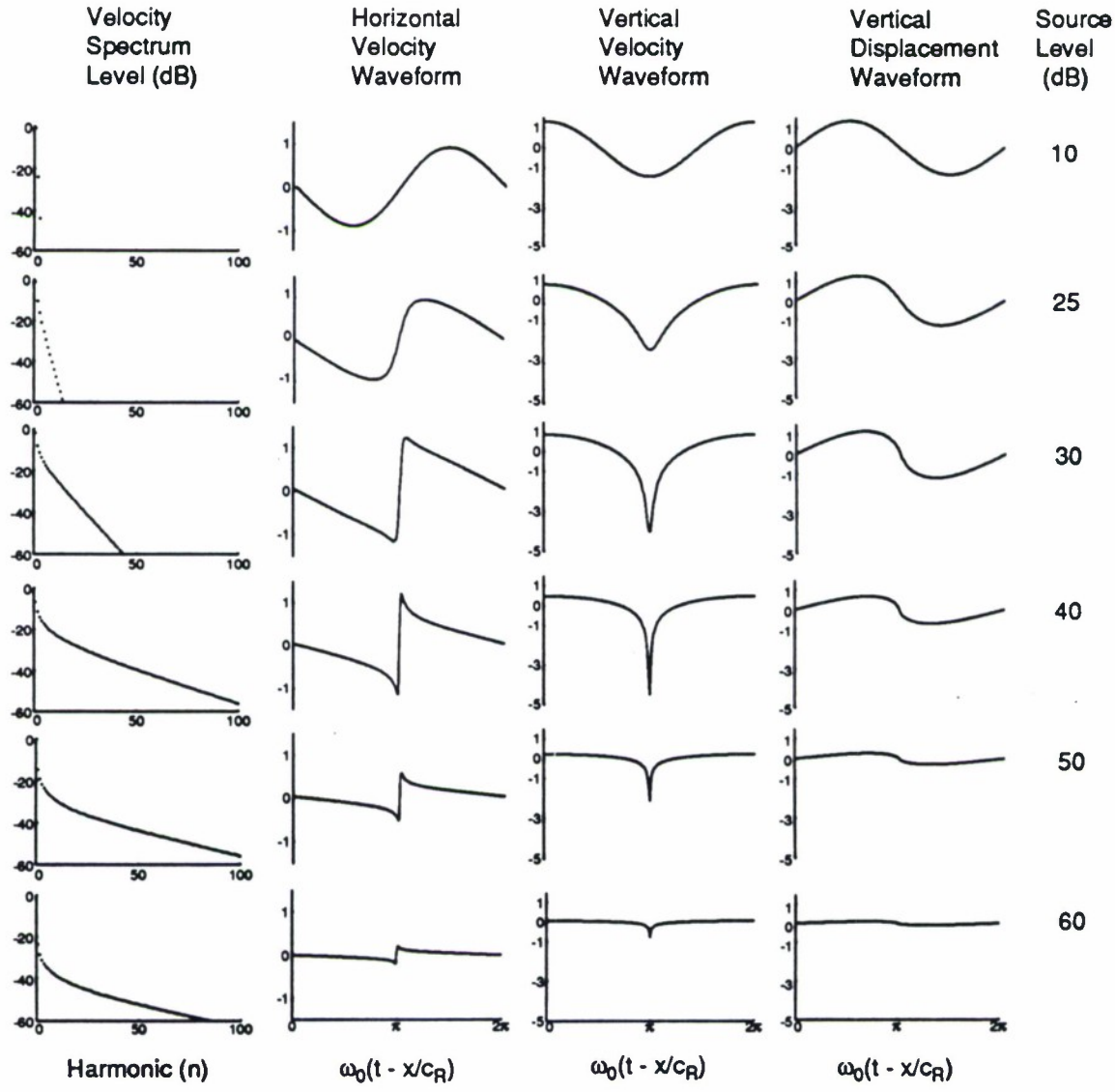

Figure 1: Predicted frequency spectra and time waveforms associated with the nonlinear distortion and acoustic saturation of a Rayleigh wave, as a function of source level.

to frequency, the harmonic generation that accompanies waveform distortion tends to localize the total energy in the wave increasingly closer to the surface.[1] When the source level is increased another 10 dB, to $L_0 = 50$ dB, saturation has occurred, and the wave amplitude at the field point is now less than that at the source because of increased losses at the shocks. Further increase in source level merely increases these losses, but the profile of the waveform remains the same. In the third column are shown the vertical velocity waveforms (which are the Hilbert transforms of the horizontal velocity waveforms), and in the fourth column are shown the vertical displacement waveforms (which are the integrals of the vertical velocity waveforms).

The second investigation examines whether stationary nonlinear planar Rayleigh waves [i.e., for which $dV_n/dR = 0$ with $m = 0$ and $A_n = 0$ in Eq. (1)] can exist.[3] Their existence has been predicted by Parker and Talbot,[4-7] who suggest that the nonlocal character of nonlinear Rayleigh waves provides a possible mechanism for the existence of nondistorting waveforms. Parker and Talbot used numerical solutions of a model equation that is similar in form to Eq. (1) to support the proposed existence of nonlinear Rayleigh waves. However, we have found that results based on Eq. (1) with $dV_n/dR = 0$ and $m = 0$ do not support their conclusions.

Figure 2(a) shows a typical computed "stationary" spectrum which was limited to $N = 50$ harmonics. The corresponding horizontal velocity waveform is shown in Fig. 2(b) (which reveals Gibbs oscillations due to the abrupt truncation of the frequency spectrum). If N can be chosen sufficiently large that no further increase in N introduces a change in either the spectrum or the waveform, then one may claim that a stationary waveform has been identified numerically (this was the procedure followed by Parker and Talbot). However, this limit can never be achieved, as was proved both analytically and numerically in Ref. 3. For example, doubling N to $2N$ will produce a spectrum with exactly the same spectral envelope as in Fig. 2(a) (when renormalized to the harmonic scale 1 to $2N$) but with twice the spectral density. In other words, there will still be three "spectral nulls," but they will now be evenly spaced between the first and hundredth harmonic, rather than the first and fiftieth. The waveform obviously changes in this case (the pulse-like shape of the waveform becomes narrower because of the higher frequency content). In conclusion, a stationary wave solution cannot be obtained on the basis of Eq. (1).

The investigation of stationary waves is completed and the results have been submitted for publication.[3] The work associated with Fig. 1 will be submitted for publication, and it is currently being extended to diffracting Rayleigh wave beams.

The third investigation produced a major new result. In particular, a method was discovered by which Eq. (1) can be rewritten in the time domain as an evolution equation (analogous to the Burgers equation for finite amplitude sound in fluids). This work is still in progress, and therefore details will be presented in the Fifth Annual Summary Report (i.e., next year). Here, we identify only the main features

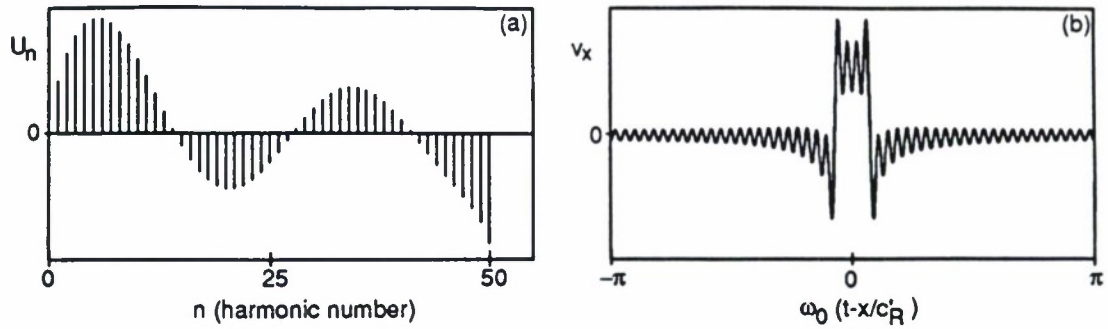

Figure 2: Numerical solution for a stationary wave with three spectral nodes, for $m = A_n = 0$ and $N = 50$: (a) frequency spectrum and (b) horizontal velocity waveform.

of the result. The nonlinearity coefficient matrix may be written as the summation[1] $C_{mn} = C^{\alpha}_{mn} + C^{\beta}_{mn} + C^{\gamma}_{mn}$. Each of the three terms alone produces nonlinear distortion effects which lead to waveforms having the same profiles as in Fig. 1. The nonlinear evolution equation associated with the third term is the easiest to derive, and it is given in dimensionless form by

$$\frac{\partial D}{\partial R} + \frac{mD}{2R} - A\frac{\partial^2 D}{\partial T^2} = \left(\frac{\partial D}{\partial T}\right)^2 + (1 - i\mathcal{H})\left(\frac{\partial D}{\partial T}\frac{\partial D^*}{\partial T} + D\frac{\partial^2 D^*}{\partial T^2}\right) \qquad (4)$$

where D^* is the complex conjugate of the *displacement* variable D, T is time, A is an attenuation coefficient, and $\mathcal{H}$ is the Hilbert transform operator. The real part of the complex function D is proportional to the horizontal component of the particle displacement, and the imaginary part is proportional to the vertical component. A computer program has been written to solve Eq. (4), and the results are indistinguishable from those obtained by solving Eq. (1) with $C_{mn} = C^{\gamma}_{mn}$ and $A_n = n^2 A_1$. It can be shown that when the Burgers equation is rewritten in terms of the complex displacement variable D, the result is identical in form to Eq. (4) apart from the absence of the term $D(\partial^2 D^*/\partial T^2)$. This term accounts for the nonlocal nonlinearity associated with Rayleigh waves (which is responsible for the cusping near the shocks in the horizontal velocity waveforms in Fig. 1).

II. Finite Amplitude Pulses in Liquids with Strong Absorption

The numerical work for this project was performed by Y.-S. Lee, the experimental work by M. A. Averkiou. Additional financial support was provided by the Packard Foundation and the National Science Foundation. Computing resources were provided by The University of Texas System Center for High Performance Computing.

The numerical work by Lee was described briefly in the Third Annual Summary Report[8] under the present ONR grant, and subsequently reported in the Proceedings of Ultrasonics International 91.[9] The following abstract appeared at the May 1992 Meeting of the Acoustical Society of America in Salt Lake City:[10]

> Measurements of intense acoustic pulses generated by directive sources in a liquid with strong absorption are compared with theoretical predictions based on a time domain numerical solution of the KZK nonlinear parabolic wave equation [obtained previously by Lee and Hamilton[9]]. The computer program is useful for describing the propagation of tone bursts with various amplitude and frequency modulations. Experiments were performed in glycerin with narrowband pulses having center frequencies of several megahertz. The pulses experience self-demodulation that leads to farfield waveforms characterized by the low frequency envelope, as predicted by the asymptotic theory of Berktay.[11] Good agreement between theory and experiment was obtained for amplitude modulated tone bursts, not only at farfield axial positions as achieved first by Moffett et al.,[12] but also off axis, throughout the transition region and into the nearfield. The effects of frequency modulation are also discussed.

An acceleration under this ONR grant provided for the purchase of a LeCroy 9112 arbitrary function generator (12 bits dynamic range, 20 nsec/point output rate). This high precision function generator has made possible a detailed study of nonlinear effects in pulsed sound beams. An example of experiment and theory is presented in Fig. 3. The pulse has a center frequency of 3.5 MHz and was produced with a 1.3 cm diameter source. Glycerin was selected as the medium because of its high absorption (approximately 6 dB/cm at 3.5 MHz), which is required to investigate self-demodulation within the dimensions of the ultrasonic tank facility in the Mechanical Engineering Department. The decibel levels cited next to each waveform indicate level relative to that at the source, and the dimensionless distance $\sigma = z/z_0$ is in terms of the Rayleigh distance z_0 at 3.5 MHz. Results from theory and experiment are seen to be in outstanding agreement, which attests to the precision of both the Mechanical Engineering tank facility and the numerical code. The slight asymmetry of the final experimental waveform is attributed to slight asymmetry in the response of the source transducer (namely, the ringing associated with the high Q), which was not taken into account in the theoretical predictions. The results in Fig. 3 represent the first instance in which theory and experiment for self-demodulation have been compared at distances before the final demodulated waveform (in the bottom row) has been established.

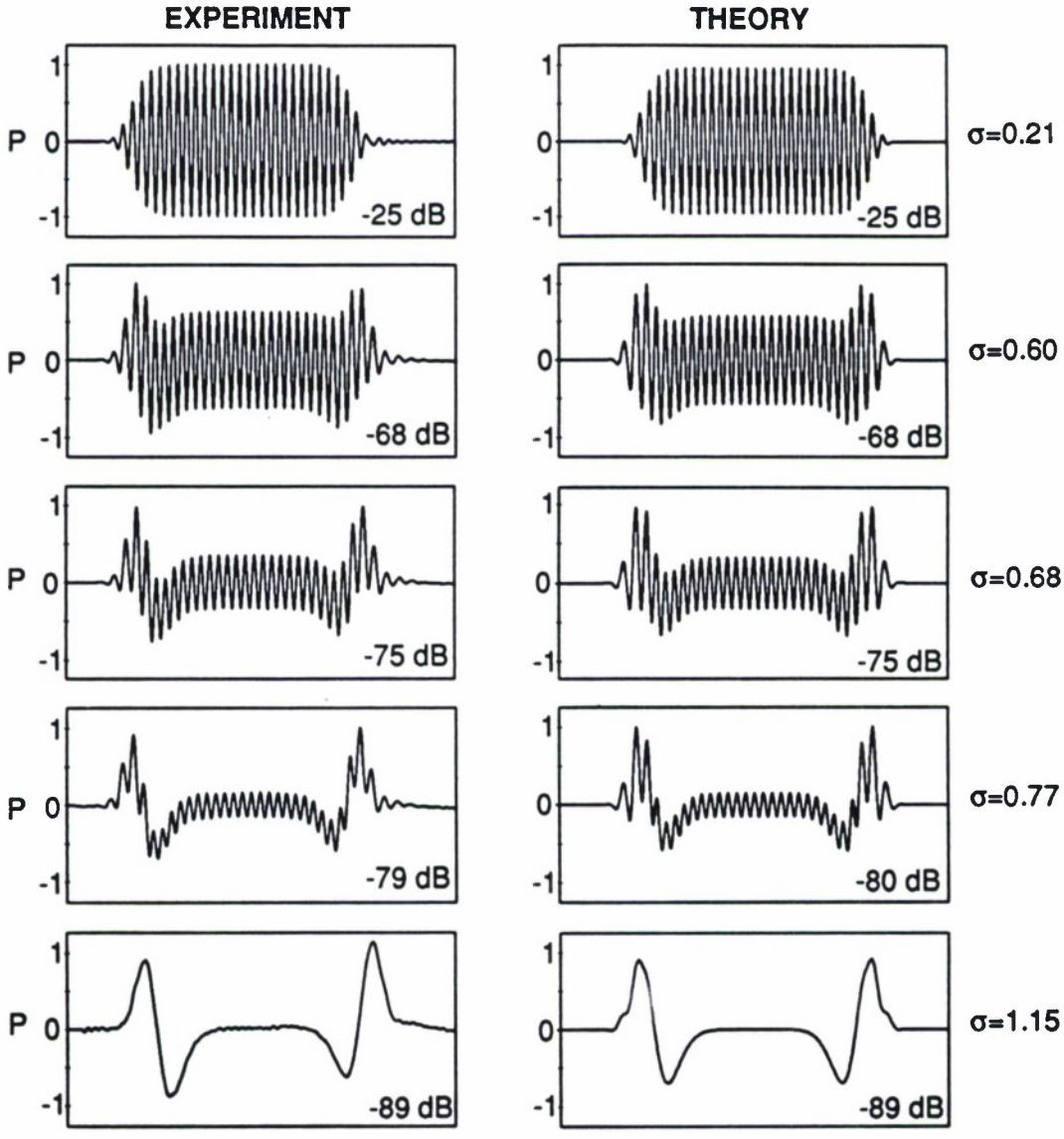

Figure 3: Comparison of theory and experiment for the self-demodulation of a 3.5 MHz tone burst in glycerin.

III. Reflection of a Focused Beam from a Curved Target

This work was performed by M. A. Averkiou, who received additional financial support from the Packard Foundation and the National Science Foundation. The work was reported at the May 1992 Meeting of the Acoustical Society of America in Salt Lake City.[13] The abstract of that presentation follows:

> The reflection of focused sound beams from surfaces with spherical curvature is investigated theoretically and experimentally. Theoretical predictions for the incident and reflected beams are based on the parabolic wave equation. A circular source with a uniform amplitude and quadratic phase distribution is assumed. Solutions for the reflected beam are derived for both pulsed and continuous sources. The experiments were performed in water with a 3.5 MHz source that has a nominal radius of 2.5 cm and focal length of 15 cm. Accurate measurements of the incident beam, particularly very near the source, were used to characterize the effective radius and focal length. Reflection from both convex and concave surfaces was investigated. The targets were made of nickel with radii of curvature that vary from 5 cm up to infinity (planar targets). Measurements of the reflected beam were obtained with a needle hydrophone that passed through a small hole in the center of the source. Agreement between theory and experiment is excellent, and the results suggest novel ways to measure surface curvature.

The theory is based on a solution for the reflection of a pulsed, focused sound beam from a rigid spherical target. For simplicity, we present here only the solution for the case in which the axis of the beam passes through the center of the target:

$$p_r/p_0 = \frac{f(\tau) - f(\tau - \tau_r)}{1 - z/d + 2b^{-1}(z - z_r)(1 - z_r/d)} \tag{5}$$

where p_0 is the pressure amplitude at the source, $f(t)$ is the source waveform, $\tau = t - z/c_0$ is retarded time in terms of the coordinate z along the axis of the beam, d is the focal length of the source, b is the radius of curvature of the target, $z = z_r$ is where the axis of the beam intersects the target, and

$$\tau_r = \frac{a^2}{2c_0}\left(\frac{1 - z/d + 2b^{-1}(z - z_r)(1 - z_r/d)}{z + 2b^{-1}z_r(z - z_r)}\right) \tag{6}$$

where a is the source radius. The solution is written in terms of an "unfolded geometry," in which the beam is assumed to propagate in the positive z direction following reflection from the target. This geometry also facilitates the presentation of data. For example, for a planar target ($b = \infty$) the solution for p_r reduces to the freefield solution for a focused beam in the parabolic approximation. Modification

of Eq. (5) to account for a geometry in which the center of the target does not coincide with the beam axis is straightforward.

Shown in Fig. 4 are comparisons of theory with experiment for the amplitude of a sinusoidal source waveform that is reflected from either a convex target ($b = +d$) or a concave target ($b = -d$). The experiment was performed in water, and the reflected pressure was measured in the center of the source, which corresponds to the location $z = 2z_r$ (i.e., twice the round trip distance from the source to the target). The receiver consisted of a small needle hydrophone inserted in the center of the source (the source radius was $a = 2.5$ cm, and its focal length was $d = 15.2$ cm). The vertical axes in Fig. 4 correspond to pressure amplitude (maximized by its maximum value), the horizontal axes to the distance between the source and the target. If the target were planar, the received pressure amplitude would be maximized with a source/target separation given by $z_r/d = 0.5$, i.e., when the target is one half focal length away from the source (because the received signal has traveled a round-trip distance d). The arrows in the figure indicate this position and provide a point of reference for comparison with results for curved targets. For the concave target ($b = -d$), the maximum is measured at $z_r/d < 0.5$ (because the target enhances the focusing effect and thus causes the beam to focus within a shorter distance, i.e., the net focal length decreases). For the convex target ($b = +d$) the maximum is measured at $z_r/d > 0.5$ (because the target defocuses the beam and thus increases the net focal length). Theory and experiment are seen to be in very good agreement. The oscillations in the response curves are due to diffraction, specifically, the interference of the center wave and edge wave radiated by the source. These contributions are represented by the two terms in the numerator of Eq. (5).

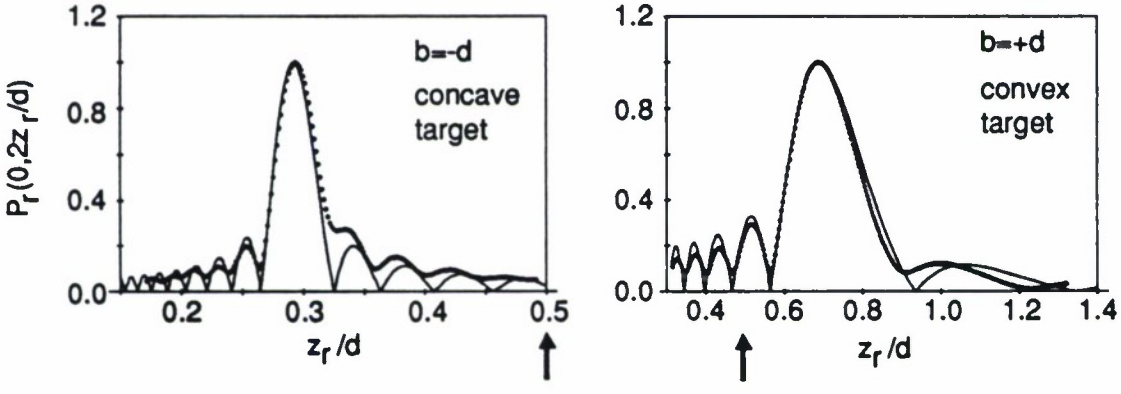

Figure 4: Comparison of linear theory and experiment for the reflection of a focused sound beam from either a concave target ($b = -d$) or a convex target ($d = +b$). The point receiver is mounted in the center of the source transducer.

The experiments reported here will be extended to the more general case of transmission and reflection at a curved fluid-fluid interface, for both finite ampli-

tude as well as for small signal sound beams.

IV. Finite Amplitude Propagation in a Sound Velocity Channel

The personnel working on this project were Ensign D. E. Reckamp, USN, and E. A. Zabolotskaya. The main financial support for Reckamp was provided by an Applied Research Laboratories Naval Academy Scholarship. Reckamp reported this work in his M.S. thesis.[14] He received an M.S. degree in Mechanical Engineering in May 1992. Apart publication of the results in a journal article, this project is completed. Additional financial support was provided by the Packard Foundation.

Background on the project is discussed in the Third Annual Summary Report[8] under the present ONR grant. The results were presented at the May 1992 Meeting of the Acoustical Society of America in Salt Lake City. The following is the abstract[15] that accompanied the presentation:

> The propagation of finite amplitude sound in a waveguide with a parabolic sound velocity profile is investigated theoretically. It is assumed that the primary wave propagates in a single mode at a frequency that is large compared with the cutoff frequency. The acoustic energy is therefore concentrated near the axis of the sound channel. Both the primary wave and the nonlinearly generated second harmonic component have mode shapes that are described by Gauss-Hermite eigenfunctions. For a primary wave in mode m, the second harmonic component is generated in all even order modes up to $2m$, with most of the energy contained in mode $2m$. A nonlinear Schrödinger equation is derived for the envelope of a narrowband pulse that propagates in a single mode. Analytical expressions are derived for the coefficients in the Schrödinger equation, and it is found that only dark envelope solitons can propagate without distortion in the waveguide.

The mode shapes of the second harmonic component were presented in the Third Annual Summary Report.[8] Below, we present the general results.

The governing wave equation is the following modified Westervelt equation:

$$\nabla^2 p - \left(\frac{1}{c_0^2} - \mu^2 z^2\right) \frac{\partial^2 p}{\partial t^2} = -\frac{\beta}{\rho_0 c_0^4} \frac{\partial^2 p^2}{\partial t^2} \tag{7}$$

where z is depth in the water column and μ characterizes the curvature of a parabolic sound velocity profile about the waveguide axis at $z = 0$ (see Fig. 5). This sound speed profile is frequently used to model the SOFAR channel. The limitations of Eq. (7) are that the acoustic wavelengths must be short compared with

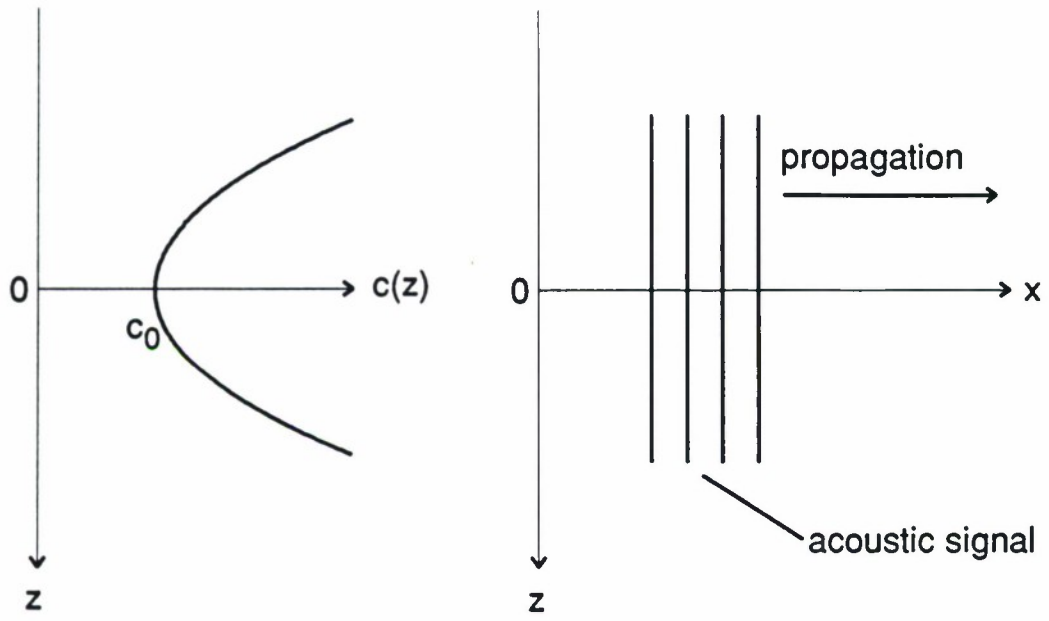

Figure 5: Coordinate system for the parabolic sound velocity channel.

the characteristic dimension of the channel (i.e., the effective width of the waveguide), and that the sound must be trapped near the waveguide axis (which means the source frequency must be several times the cutoff frequency). If it is further assumed that the primary sound field consists of a single frequency ω and propagates in a single mode m, the following quasilinear solutions are obtained for the fundamental (p_1) and second harmonic (p_2) pressure components:

$$p_1 = p_0 e^{-\mu\omega z^2/2} H_m\left(z\sqrt{\mu\omega}\right) e^{j(\omega t - k_m x)} \tag{8}$$

$$p_2 = \frac{j2\omega\beta p_0^2}{2^m \mu\rho_0 c_0^4} e^{-\mu\omega z^2} H_{2m}\left(z\sqrt{2\mu\omega}\right) \sin\left[\left(\kappa_m - k_m\right) x\right] e^{j[2\omega t - (\kappa_m + k_m)x)} \tag{9}$$

where k_m is the wavenumber of the fundamental component, $2\kappa_m$ is the axial wavenumber of a freely propagating second harmonic component, and H_m is the Hermite polynomial of order m. The expression for p_1 is well known,[16] whereas the expression for p_2 is new. Because the fundamental and second harmonic components propagate at different speeds in the waveguide ($k_m \neq \kappa_m$), the amplitude of the second harmonic component experiences spatial beating. The spatial periodicity of the beating is $\pi/(\kappa_m - k_m) \simeq 4\pi/\mu c_0$. The expression for p_2 is a single mode approximation. The full expression for p_2 includes $m+1$ modes, i.e., all even modes from 0 through $2m$. However, it was discovered that most of the energy is contained in the highest mode, $2m$, which provides justification for the single mode approximation.

The propagation of narrowband pulses was also considered. The expression for a narrowband pulse that propagates in a single mode may be written

$$p_1 = a(x,\tau)e^{-\mu\omega_0 z^2/2}H_m\left(z\sqrt{\mu\omega_0}\right)e^{j(\omega_0 t - k_m x)} \tag{10}$$

where ω_0 is the center frequency of the pulse, a is the pulse envelope function, $\tau = t - x/c_g$ is a retarded time, and c_g the group velocity of the pulse. A nonlinear Schrödinger equation (NLS) can be derived for waveguides:[17]

$$j\frac{\partial a}{\partial x} + \frac{k_m''}{2}\frac{\partial^2 a}{\partial \tau^2} + \Lambda|a|^2 a = 0 \tag{11}$$

where $k_m'' = d^2k_m/d\omega_0^2$. The NLS predicts the existence of envelope solitons, bright solitons if $\Lambda/k_m'' > 0$ or dark solitons if $\Lambda/k_m'' < 0$. The case $\Lambda/k_m'' < 0$ also indicates that localized energy packets (i.e., which vanish as $\tau \to \pm\infty$) will disperse as they propagate. An analytical expression was derived for the ratio Λ/k_m'' in the single mode approximation for the second harmonic component:[14]

$$\frac{\Lambda}{k_m''} = -\frac{\sqrt{2}(2m)!\beta^2\omega_0^5(1-\omega_m/\omega_0)}{2^{2m}(m!)^2(2m+1)^2\sqrt{\pi}\mu^3\rho_0^2c_0^{10}} \tag{12}$$

where ω_m is the cutoff frequency for the pulse ($\omega_0 > \omega_m$ is assumed). This expression is always negative, which means that bright solitons cannot exist in this waveguide, and pulses will disperse as they propagate.

V. Second Harmonic Generation in Pekeris Waveguides

This work was performed by C. E. Bruch, Yu. A. Il'insky, and E. A. Zabolotskaya, who each received additional financial support from the Packard Foundation. Further background information on this project may be found in the Third Annual Summary Report.[8]

The Pekeris[18] waveguide model consists of two liquid layers having different sound speeds. The upper layer ($0 \le z \le h_1$) is bounded above by a free surface at $z = 0$ and below ($z > h_1$) by a second, penetrable layer. The lower layer is usually assumed to have infinite depth ($h_2 = \infty$). When the sound speed in the lower layer exceeds that in the upper layer ($c_2 > c_1$, where the index 1 refers to the upper layer and the index 2 to the lower layer), guided wave propagation can exist in the upper layer. This is the situation for sea water over sediment. Although the Pekeris waveguide model has been widely used to study the acoustics of shallow ocean channels in the small signal approximation,[16] no analyses have been reported on finite amplitude effects. Here we present preliminary results for second harmonic generation in a Pekeris waveguide.

In the course of the investigation, it proved useful to consider a slightly modified version of the Pekeris waveguide model. In particular, a lower layer of finite, rather

than infinite, depth was assumed ($h_1 < h_2 < \infty$). The reason for this assumption is that the sound field in an infinite domain ($h_2 = \infty$) must be described with a continuous spectrum of modes (plus a discrete spectrum that corresponds to the upper layer), whereas a field in a finite domain consists of only a discrete spectrum of modes. The continuous spectrum is frequently ignored, because it contributes significantly to the acoustic field only very near the source.[16] However, analysis of second harmonic generation requires careful consideration of the field near the source, in particular, to properly match the source condition. As a practical matter, matching the source condition analytically is more easily achieved when the modes form a discrete rather than a continuous spectrum. For the case of trapped wave propagation in the upper layer, in which acoustic penetration in the lower layer is restricted to within approximately one wavelength beneath the interface, it was found that the thickness of the lower layer need only be on the order of the thickness of the upper layer ($h_2 \sim 2h_1$) to simulate an ideal Pekeris waveguide ($h_2 = \infty$).

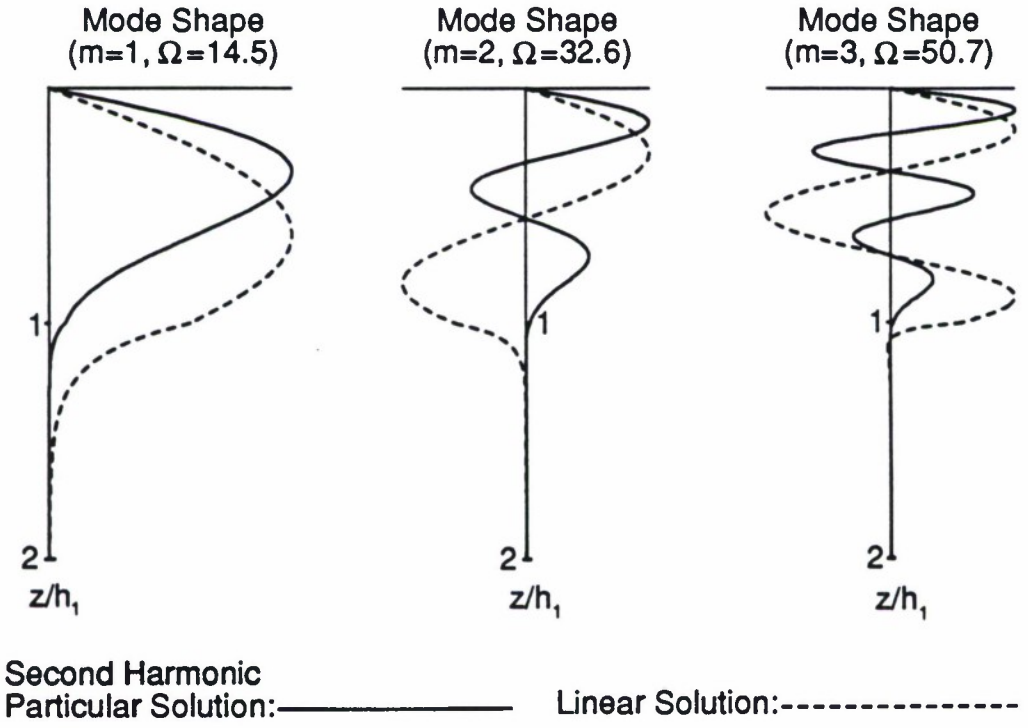

Figure 6: Predicted fundamental and second harmonic mode shapes (dashed and solid lines, respectively) in a Pekeris waveguide formed by sea water over sediment.

In Fig. 6 are shown mode shapes corresponding to second harmonic generation (solid lines) by a primary wave (dashed lines) that propagates in mode $m = 1$, 2, or 3 in a layer of sea water over sediment ($c_1/c_2 = 0.86$, $\rho_1/\rho_2 = 0.5$). The

bottom of the lower layer ($h_2 = 2h_1$) is assumed to be perfectly rigid. Only the forced component (the particular solution) of the second harmonic wave is shown in the figure. The dimensionless source frequency $\Omega = \omega c_1/h_1$ increases with mode number in such a way as to maintain a constant angle of incidence between the water-sediment interface and the propagation directions of the plane waves that constitute the mode at the source frequency. This angle is $\theta = 10°$. The critical angle for this case is $\theta_c = 30°$, which means that total internal reflection occurs in the upper layer, and the primary wave is trapped. The main observation is that the penetration depth of the nonlinearly generated second harmonic component is slightly less than at the source frequency. Otherwise, the properties of second harmonic generation due to a primary wave trapped in the upper layer of a Pekeris waveguide are similar to those for the case in which the sound in the upper layer is trapped by a rigid surface at $z = h_1$.[19] For example, second harmonic generation is slightly more efficient near the free surface than near the fluid-fluid interface.

VI. Finite Amplitude Propagation in Multiple Waveguide Modes

This work was performed by T. W. VanDoren, who received additional financial support from a Rockwell Fellowship and the Packard Foundation. Preliminary work on the project was discussed in the Third Annual Summary Report.[8]

The waveguide investigations described in the previous two sections of this report (Secs. IV and V) are based on the assumption that the primary wave propagates in only one mode, which results in a tremendous simplification of the analysis. Except in carefully designed experiments, however, this is usually not the case, and the primary wave propagates in a variety of modes. The purpose of the present investigation is to consider how the propagation of a primary wave in more than one mode affects harmonic generation and shock formation. The analysis proceeds as follows. First, a quasilinear analytical solution of a Westervelt nonlinear wave equation is derived for second harmonic generation in a rectangular duct with rigid walls, with the primary wave propagating in an arbitrary number of modes. Second, the corresponding quasilinear solution is derived on the basis of the parabolic (KZK) approximation of the nonlinear wave equation. Third, if these solutions (Westervelt and KZK) compare well with each other and with experiment, then existing computer programs for solving the fully nonlinear KZK equation will be modified for application to guided wave propagation.[20,21] The numerical solutions can be used to predict third and higher harmonic generation, as well as shock formation. Moreover, pulsed sound in waveguides can then be explored. Although a numerical solution of a KZK-type equation for guided finite amplitude sound has already appeared in the literature,[22] we feel that a careful analysis, based on both analytical solutions and experiment, is needed to justify this approach.

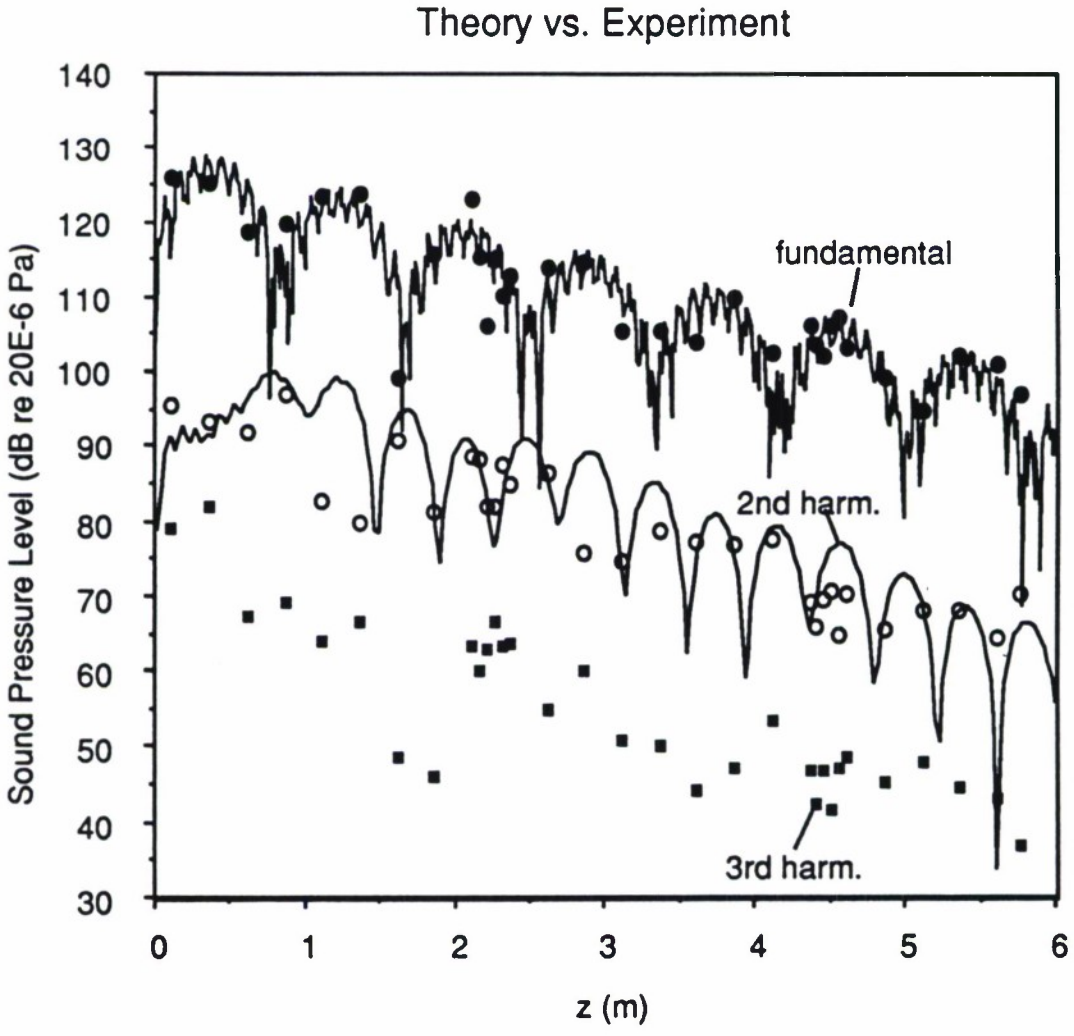

Figure 7: Comparison of quasilinear theory for second harmonic generation (solid lines) with experiment for a 33 kHz piston source in an air-filled rectangular waveguide.

Quasilinear analytical solutions for second harmonic generation by a primary wave in multiple waveguide modes were derived from both the Westervelt and KZK equations. The solutions are too cumbersome to present here. An experiment was performed in which the fundamental, second and third harmonic components were measured in an air-filled rectangular duct. The transverse dimension of the duct is 6.6 cm, and it was excited with a centered 3.3 cm, 33 kHz source that (in theory) produced sound in four propagating modes. The second harmonic should then be generated in only two propagating modes for this geometry. The results, both theory (based on the Westervelt equation with ad hoc attenuation coefficients) and experiment, are shown in Fig. 7. The agreement for the fundamental and second harmonic components, in terms of general properties, is very reasonable. No analytical solution for the third harmonic component was derived. Theoretical description of this component will be based on a numerical solution of the KZK equation.

VII. Cooperative Radiation and Scattering of Sound by Bubbles

Work on this project was performed by Il'insky and Zabolotskaya, who received additional financial support from the Packard Foundation. This research is now completed, and a journal article has been accepted for publication in the Journal of the Acoustical Society of America.[23] The results have also been presented at the May 1992 Meeting of the Acoustical Society of America in Salt Lake City.[24] The following is the abstract from that meeting:

> The process of cooperative radiation of acoustic waves by radial bubble oscillations is investigated theoretically. In addition to instantaneous bubble interaction,[25] we have also taken into account the interaction due to acoustic radiation. Numerical results for the acoustic intensity produced by 10 bubbles that pulsate in water with random initial phases are presented. Mutual bubble interaction causes synchronization of the bubble pulsation phases, which gives rise to collective radiation. The phenomenon is not as strong as in optics. In order to ensure superradiance by 10 bubbles, the radial oscillations of the bubbles must have amplitudes of the order of their initial radii.

The details of this work are summarized by the following (modified) excerpts from the forthcoming journal article.[23]

It is known that distributions of gas bubbles produce dramatic changes in the properties of a liquid. In particular, bubbles introduce strong nonlinearity and dispersion. Bubble oscillations result in the radiation of acoustic waves, and their contribution to ocean noise and sound scattering is substantial.[16]

The aforementioned phenomena are usually analyzed with the Rayleigh equation for single bubble pulsations. Cooperative effects are not taken into account, apart from the bubble contribution to the coherent part of the acoustic field that arises during sound propagation through a quasi-homogeneous mixture of a liquid with bubbles. This is the usual model of a two-phase homogeneous medium. The present work constitutes a theoretical analysis of the collective radiation and scattering of sound by bubbles. A new feature of the analysis is the inclusion of a term that takes into account the bubble interaction through the radiation field.

The following coupled dimensionless equations were derived to describe the volume oscillations of a collection of bubbles with a distribution of radii:

$$\frac{dV_n}{dT} = j\delta_n V_n - j\Gamma_n |V_n|^2 V_n - \sum_m V_m \tag{13}$$

where V_n is the (dimensionless) volume of the nth bubble, T is time, δ_n accounts for the frequency shift connected with instantaneous bubble interaction through the radiation field and the deviation of the bubble oscillation frequency from the mean frequency that characterizes the given bubble distribution, Γ_n is a coefficient that accounts for both quadratic and cubic nonlinearity, and the summation represents bubble interaction through the radiation field.

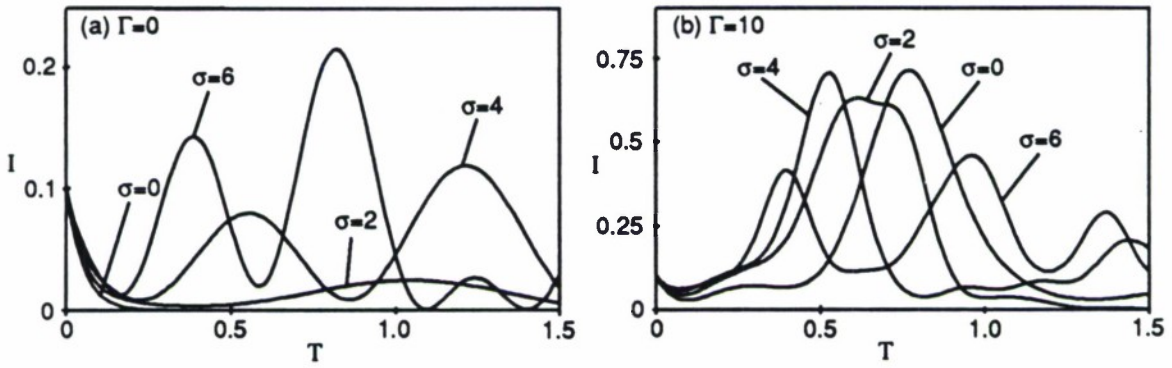

Figure 8: Intensity of sound radiated by ten oscillating bubbles as a function of time, based on (a) linear and (b) nonlinear theory. The standard deviation of the bubble radius distribution is σ.

The results of integrating Eqs. (13) are shown in Fig. 8. A field of 10 bubbles was assumed, the initial pulsation amplitudes of which were assumed to be equal. The initial phase of each bubble is arbitrary, and the phase distribution (corresponding to values of δ_n) was assigned randomly according to the standard deviations $\sigma = 0, 2, 4, 6$. The vertical axes in Fig. 8 represent $I = |\sum V_n|^2/n$, which is proportional to the radiation intensity. Figure 8(a) pertains to a linear ($\Gamma_n = 0$) solution of Eqs. (13), Fig. 8(b) to a nonlinear ($\Gamma_n = 10$) solution. Note that in the linear case,

Fig. 8(a), the intensity does not decay monotonically with time when there is a distribution of bubble sizes. Localized intensity maxima occur when the bubbles momentarily oscillate in phase as a result of their different resonance frequencies. In the nonlinear system, Fig. 8(b), the localized intensity maxima are an order of magnitude greater than in the linear case. This nonlinear acoustical phenomenon is the analog of superradiance in nonlinear optics. To achieve nonlinearity designated by $\Gamma_n = 10$, however, the bubbles must pulsate with volume amplitudes that are of the order of their initial volumes. It is therefore unlikely that a superradiance pulse will be observed in acoustics via bubble interations in liquids.

The main conclusion of this work is that cooperative effects should be taken into account when there are many bubbles in the liquid and they are sufficiently close to each other to interact. Nonlinear effects cause the bubble oscillation frequencies to depend on pulsation amplitudes, which leads to phase matching and a phenomenon analogous to superradiance in optics.

VIII. Water Fountains Produced by Intense Standing Waves in Air

This work was primarily experimental and was performed by T. W. VanDoren. VanDoren received additional financial support through a Rockwell Fellowship and from the Packard Foundation. The following abstract[26] from an oral presentation at the May 1992 Meeting of the Acoustical Society of America in Salt Lake City summarizes the motivation for this work.

> An acoustics demonstration found in several science museums involves a horizontal standing wave tube which contains a shallow layer of liquid. When the liquid is water and the sound pressure level of a standing wave in the air above the water exceeds approximately 160 dB (re 20 μPa) at frequencies below 1 kHz, vigorous fountains occur at the nodes in the pressure field. The introduction of a surfactant in the water causes clusters of fountains to appear near the nodal planes at somewhat lower sound pressure levels. Standard quasilinear theory provides a reasonable description of the acoustic streaming and dc pressure in the air prior to the appearance of fountains. The fountains seem to result from the ejection of droplets by inner streaming vortices that are formed above the air-water interface. The water fountains and streaming patterns are discussed in relation to Andrade's observations[27] of solid particulate motion produced by intense standing waves in air.

The presentation was accompanied by a videotaped visualization of the acoustic streaming in the standing wave tube. A half cylinder on one wall of the tube, rather than the small modulations produced by the surface of the water, was used

to enhance the streaming. The vizualization was performed with a laser and smoke particles. However, the inner streaming vortices that are believed to be responsible for the water fountains could not be vizualized with this technique, and only the outer streaming vortices were readily viewed. Laser doppler velocimetry was used to confirm the existence of the inner streaming layer. Whereas acoustic streaming patterns of this type (i.e., inner and outer circulations near boundaries) are well known,[28] as are water fountains produced by standing waves in air (they may be found in several science museums), the suggestion that the fountains are driven by streaming has not, to our knowledge, been discussed previously in the literature.

IX. Spark-Source Lithotripter Pulses

This work was performed mainly during the 1990–91 reporting period, as described in the Third Annual Summary Report[8] under the present ONR grant, but the comparisons of theory and experiment shown below are new. The project is now completed, and an article has been submitted for publication in the Journal of the Acoustical Society of America.[29] This work was also presented at the November 1991 Meeting of the Acoustical Society of America in Houston,[30] and it is scheduled for presentation at, and publication in the proceedings of, the 14th International Congress on Acoustics to be held in Beijing in September 1992.[31] Additional financial support was provided by the Packard Foundation.

The results may be summarized with the following abstract from the submitted journal article:[29]

> A transient solution is derived for the reflected pressure field along the axis of symmetry of a concave, axisymmetric, ellipsoidal mirror. The incident field is a spherical wave produced at the near focus of the mirror. Short wavelengths in comparison with the minimum radius of curvature of the mirror, and lossless, small signal propagation in a homogeneous fluid are assumed. The pressure at the far focus is given by a simple analytical solution, and elsewhere along the axis by a convolution integral. The results constitute a generalization of the theory developed for spherical mirrors by Cornet and Blackstock.[32] Application to waveforms produced by spark-source lithotripters is discussed, and comparisons are made with measurements reported by Müller.[33]

The axial solution for the reflected pressure p_2 can be written in the form

$$\frac{p_2}{p_0} = H_c(z)f(\tau_c) + H_e(z)f(\tau_e) + \frac{c_0}{a}\int_{t_1}^{t_2} H_w(z,t')f(t-t')\,dt' \qquad (14)$$

where p_0 is the pressure amplitude and $f(t)$ the time dependence of the source waveform. The first term is associated with the *center wave*, the second term

with the *edge wave*, and the third term with the *wake*. The corresponding impulse response functions H_c, H_e and H_w are defined in Refs. 29 and 31.

For the calculations in Fig. 9 we considered a half ellipse with eccentricity $\epsilon = 0.7$ (and therefore a far focus at $z/a = 0.7$). The source waveform $f(t)$ is shown in Fig. 9(a). The parameters approximate those of an experiment performed in water by Müller,[33] whose measured waveforms (reproduced from Fig. 4 of Ref. 33) at three axial locations (z/a = 0.47, 0.75, and 0.93) appear in the left column of Fig. 9, opposite the corresponding theoretical predictions based on Eq. (14). Müller used a Dornier XL1 lithotripter, and the duration of his incident pulse was approximately $T = 4$ μsec. The pairs of vertical dashed lines in Figs. 9(c)–9(e) identify the approximate beginnings and ends of the oscilloscope traces in the left column. The label C in the figures identifies the beginning of the center wave, E identifies the beginning of the edge wave, and W identifies the most pronounced contribution due to the wake.

At $z/a = 0$, the center wave and edge wave are well separated, and the wake produces a slight negative pressure immediately following the center wave. At $z/a = 0.47$ the center wave and edge wave are still clearly resolved. Comparison of Fig. 9(c) with the oscilloscope trace to the left indicates that the small negative pressure at the end of the measured waveform is evidently due to the wake rather than the edge wave. The oscilloscope trace appears to end prior to the arrival of the edge wave. At $z/a = 0.75$, just beyond the far focus, the center wave and edge wave overlap, and the wake produces a large positive pressure. However, the predicted waveform in Fig. 9(d) appears backwards in comparison with the corresponding measured waveform. This reversal is probably due to nonlinear effects introduced by the large peak pressure, which is approximately 800 bar (80 MPa). Nonlinearity would cause point W in Fig. 9(d) to catch up with point E and thus produce a waveform more like that which was measured. Note also that the amplitude ratio of point W in Fig. 9(d) to point C in Fig. 9(c) matches the ratio of the corresponding measured peak pressures. At $z/a \doteq 0.93$, both the measured and predicted waveforms possess a horizontal plateau that follows the arrival of the edge wave (E), leading to a spike produced by the wake (W) in the middle of the waveform. Again, nonlinear effects would cause point W in the predicted waveform to advance in time relative to point E. Although the predicted amplitude ratio of point W to point E matches the measured ratio, the predicted negative pressure due to the center wave is much greater than was measured. At $z/a = 2$, the edge wave has separated from the center wave, and the effect of the wake is reduced.

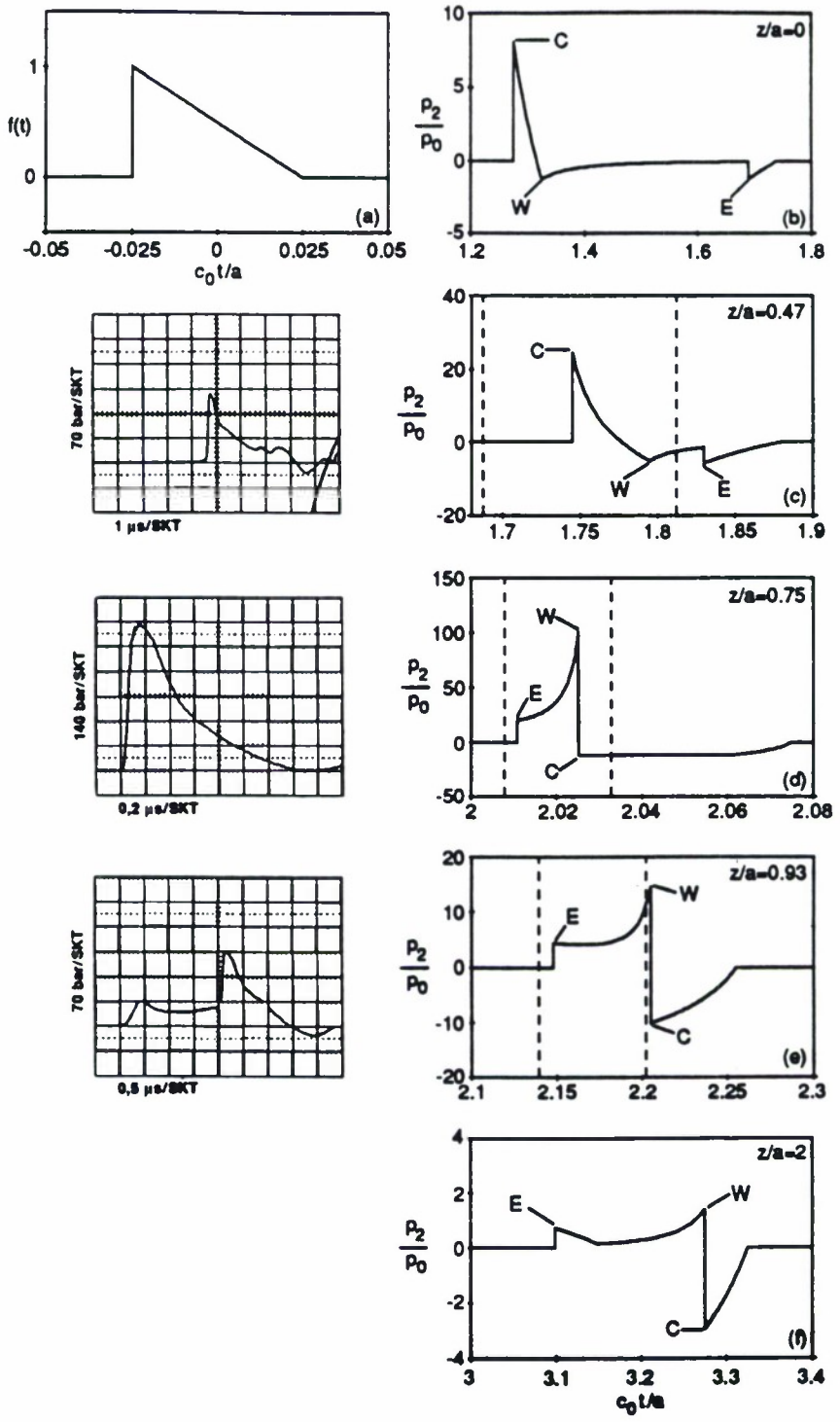

Figure 9: Comparison of present theory (right column) and experiment for lithotripsy pulses measured in water by Müller.[33]

BIBLIOGRAPHY

[1] E. A. Zabolotskaya, "Nonlinear propagation of plane and circular Rayleigh waves in isotropic solids," *J. Acoust. Soc. Am.* **91**, 2569–2575 (1992).

[2] H. M. Merklinger, "Fundamental-frequency component of a finite-amplitude plane wave," *J. Acoust. Soc. Am.* **54**, 1760–1761 (1973).

[3] M. F. Hamilton, Yu. A. Il'insky, and E. A. Zabolotskaya "On the existence of stationary nonlinear Rayleigh waves," *J. Acoust. Soc. Am.* (in review).

[4] D. F. Parker and T. M. Talbot, "Nonlinear elastic surface waves," in *Nonlinear Deformation Waves*, edited by V. Nigul and J. Engelbrecht (Springer, Berlin, 1983), pp. 397–403.

[5] D. F. Parker and T. M. Talbot, "Analysis and computation for nonlinear elastic surface waves of permanent form," *J. Elast.* **15**, 389–426 (1985).

[6] D. F. Parker, "Waveform evolution for nonlinear surface acoustic waves," *Int. J. Engng. Sci.* **26**, 59–75 (1988).

[7] D. F. Parker, "Nonlinear surface acoustic waves on homogeneous media," in *Nonlinear Waves in Solid State Physics*, edited by A. D. Boardman, M. Bertolotti, and T. Twardowski (Plenum Press, New York, 1990), pp. 163–193.

[8] M. F. Hamilton, "Problems in nonlinear acoustics," Third Annual Summary Report under ONR Grant N00014-89-J-1003, Department of Mechanical Engineering, The University of Texas at Austin, August 1991.

[9] Y.–S. Lee and M. F. Hamilton, "Nonlinear effects in pulsed sound beams," Ultrasonics International 91 Conference Proceedings (Butterworth-Heinemann, Oxford, 1991), pp. 177–180.

[10] M. A. Averkiou, Y.–S. Lee, and M. F. Hamilton, "Propagation of pulsed finite amplitude sound beams in a liquid with strong absorption," *J. Acoust. Soc. Am.* **91**, 2455 (1992).

[11] H. O. Berktay, "Possible exploitation of non-linear acoustics in underwater transmitting applications," *J. Sound Vib.* **2**, 435–461 (1965).

[12] M. B. Moffett, P. J. Westervelt, and R. T. Beyer, "Large amplitude pulse propagation—A transient effect," *J. Acoust. Soc. Am.* **47**, 1473–1474 (1970).

[13] M. A. Averkiou and M. F. Hamilton, "Reflection of focused sound beams from curved surfaces," *J. Acoust. Soc. Am.* **91**, 2470 (1992).

[14] D. E. Reckamp, "Propagation of finite amplitude sound in a waveguide with a parabolic sound velocity profile," M.S. Thesis, The University of Texas at Austin (May 1992).

[15] D. E. Reckamp, E. A. Zabolotskaya, and M. F. Hamilton, "Propagation of finite amplitude sound in a waveguide with a parabolic sound velocity profile," *J. Acoust. Soc. Am.* **91**, 2352 (1992).

[16] I. Tolstoy and C. S. Clay, *Ocean Acoustics* (Acoustical Society of America, New York, 1987).

[17] E. A. Zabolotskaya and A. B. Shvartsburg, "Nonlinear acoustic waveguide," *Sov. Phys. Acoust.* **34**, 493–495 (1988).

[18] C. L. Pekeris, "Propagation of explosive sound in shallow water," *Geol. Soc. Am. Mem.* **27**, Paper 2, 1–117 (1948).

[19] M. F. Hamilton and E. A. Zabolotskaya, "Nonlinear propagation of sound in a liquid layer between a rigid and a free surface," *J. Acoust. Soc. Am.* **90**, 1048–1055 (1991).

[20] J. Naze Tjøtta, S. Tjøtta, and E. Vefring, "Propagation and interaction of two collinear finite amplitude sound beams," *J. Acoust. Soc. Am.* **88**, 2859–2870 (1990).

[21] E. E. Kim, "Nonlinear effects in asymmetric cylindrical sound beams," M.S. Thesis, The University of Texas at Austin, 1990.

[22] J. J. Ambrosiano, D. R. Plante, B. E. McDonald, and W. A. Kuperman, "Nonlinear propagation in an ocean acoustic waveguide," *J. Acoust. Soc. Am.* **87**, 1473–1481 (1990).

[23] Yu. A. Il'insky, and E. A. Zabolotskaya, "Cooperative radiation and scattering of acoustic waves by gas bubbles in liquids," *J. Acoust. Soc. Am.* (in press).

[24] Yu. A. Il'insky and E. A. Zabolotskaya, "Cooperative radiation of acoustic waves by gas bubbles in a liquid," *J. Acoust. Soc. Am.* **91**, 2351 (1992).

[25] E. A. Zabolotskaya, "Interaction of gas bubbles in a sound field," *Sov. Phys. Acoust.* **30**, 365–368 (1984).

[26] T. W. VanDoren and M. F. Hamilton, "Water fountains produced by intense standing waves in air," *J. Acoust. Soc. Am.* **91**, 2330 (1992).

[27] E. N. Andrade, "On the groupings and general behaviour of solid particles under the influence of air vibrations in tubes," *Proc. Roy. Soc.* **230A**, 413–445 (1932).

[28] W. L. Nyborg, "Acoustic Streaming," in *Physical Acoustics*, Vol. IIB, edited by W. P. Mason (Academic Press, New York, 1965), pp. 265–331.

[29] M. F. Hamilton, "A transient axial solution for the reflection of a spherical wave from a concave ellipsoidal mirror," *J. Acoust. Soc. Am.* (in review).

[30] M. F. Hamilton, "An axial solution for the reflection of a spherical wave from a concave ellipsoidal mirror," *J. Acoust. Soc. Am.* **90**, 2340 (1991).

[31] M. F. Hamilton, "A transient solution for the axial pressure field of a spark-source lithotripter," to appear in *Proceedings of the 14th International Congress on Acoustics* (Beijing, China, September 1992).

[32] E. P. Cornet and D. T. Blackstock, "Focusing of an N wave by a spherical mirror," *J. Acoust. Soc. Am.* **52**, 115 (1972). See also E. P. Cornet, "Focusing of an N wave by a spherical mirror," Tech. Rep. ARL-TR-72-40, Applied Research Laboratories, The University of Texas at Austin (1972).

[33] M. Müller, "Comparison of Dornier lithotripters: Measurement of shock wave fields and fragmentation effectiveness," *Biomed. Technik* **35**, 250–262 (1990) (in German).